PORTLAND PRESS

Review Article

Driving antimalarial design through understanding of target mechanism

Petar P. S. Calic[1],*, Mahta Mansouri[1],*, Peter J. Scammells[1] and Sheena McGowan[2]

[1]Medicinal Chemistry, Monash Institute of Pharmaceutical Sciences, Monash University, Parkville, VIC 3052, Australia; [2]Department of Microbiology, Biomedicine Discovery Institute, Monash University, Clayton, VIC 3800, Australia

Correspondence: Sheena McGowan (sheena.mcgowan@monash.edu)

OPEN ACCESS

Malaria continues to be a global health threat, affecting approximately 219 million people in 2018 alone. The recurrent development of resistance to existing antimalarials means that the design of new drug candidates must be carefully considered. Understanding of drug target mechanism can dramatically accelerate early-stage target-based development of novel antimalarials and allows for structural modifications even during late-stage preclinical development. Here, we have provided an overview of three promising antimalarial molecular targets, *Pf*DHFR, *Pf*DHODH and *Pf*A-M1, and their associated inhibitors which demonstrate how mechanism can inform drug design and be effectively utilised to generate compounds with potent inhibitory activity.

Introduction

Malaria is caused by an infection with the apicomplexan parasite of the genus *Plasmodium*. An estimated 219 million cases and 405 000 malaria-induced fatalities occurred in 2018 alone, with children under age 5 representing two-thirds of these incidences [1]. Resistance to existing antimalarials, particularly to WHO recommended artemisinin combination therapies (ACTs), has been attributed as one of the major reasons that progress toward malaria elimination has slowed in many developing nations [1,2]. The first clinical signs of resistance to ACT in *Plasmodium falciparum* (*Pf*) malaria was reported in 2004 in Cambodia and raised concerns as there are no alternative first-line treatments of *Pf* available [3,4]. The recurrence of resistance, coupled with the slowly rising incident rate (2% since 2015) means that the design of novel antimalarials needs to be carried out in an efficient and rational manner.

For the last few decades phenotypic-based high-throughput screening (HTS) has been particularly useful for neglected and orphan diseases [5]. Molecules from these screens are typically first-in-class medicines often with unknown mechanism of action (MoA) that play an important role in the design of follower drugs [6]. Phenotypic screening can reduce the time between candidate identification and preclinical trials, and can guarantee that a molecule has the ability to permeate membranes [5]. These candidates can struggle in later stages of development as limited mechanistic information restricts the capacity to re-design if toxicity or selectivity issues arise [7]. In contrast, target-based campaigns rely heavily on knowledge of the target structure, function and MoA to design new inhibitors. A detailed understanding of the structure activity relationships (SAR), achievable through data from *in vitro* target-based assays and structural biology techniques such as X-ray crystallography and cryo-electron microscopy, allows researchers to fine-tune a drug candidate to optimise the desired properties. When structural data is available, target-based approaches can also utilise vast libraries of hit candidates via *in silico* screening, which require fewer resources than a quintessential HTS.

In this review, we have explored three examples of target-based campaigns, which are all currently in different stages of development, to show how knowledge of target mechanism in these programs have accelerated antimalarial design. Each program has taken advantage of structure-function data to inform the design of candidate molecules as well as to overcome disadvantages of the associated

*These authors contributed equally to this work.

biological targets. Our first example is the pyrimethamine-resistant target dihydrofolate reductase (DHFR), which has undergone an extensive target-based program that has resulted in a number of inhibitors, including the Medicines for Malaria Venture (MMV) clinical candidate **P218**. Our second example demonstrates how structural data provided a route to selective and potent inhibitors of plasmodial dihydroorotate dehydrogenase (DHODH). Finally, we explore an early drug discovery program focused on the *Plasmodium* M1 aminopeptidases (*Pf*A-M1) and the various structure-based campaigns which allowed for the design and synthesis of potent cross-species inhibitors. These examples aim to highlight that target-based drug design approaches play an important role in the future of antimalarial research.

Dihydrofolate reductase — A resistant enzyme made sensitive

Dihydrofolate reductase has a vital role in cell growth and proliferation by catalysing the reduction in dihydrofolic acid to tetrahydrofolic acid. Tetrahydrofolic acid is a folic acid (folate) derivative and is required in *Pf* for the synthesis of deoxythymidine monophosphate, a DNA monomer [8]. In protozoa, the DHFR protein encodes a thymidylate synthase (TS) domain resulting in a bifunctional enzyme, in contrast with human DHFR where the two enzymes are separate [9]. *Pf*DHFR-TS (Figure 1A) exists as a dimer, with each monomer 608 residues in length, with an N-terminal DHFR domain of 231 residues (in cyan, Figure 1A) and a C-terminal TS domain of 288 residues (in orange, Figure 1A). The two enzymatic domains are connected by an 89 amino acid junction region (in pink, Figure 1A) [10]. The DHFR domain consists of an eight-stranded central β-sheet surrounded by seven α-helices. The wild-type (WT) active site includes Ile14, Ala16, Trp48, Asp54, Phe58, Ser108, Ile164 and Thr185, which interact with both dihydrofolic acid and NADPH, a cofactor that acts as an electron donor (Figure 1B) [10].

Some of the earliest synthetic antimalarials targeted DHFR [11–15]. Cycloguanil (**1**) and pyrimethamine (Pyr) (**2**), date back to the 1940s [16,17] but long-term widespread use of these molecules has led to resistance through the evolution of multiple mutations in *Pf*DHFR [18–20]. The problematic *Pf*DHFR 'quadruple mutant' (QM) has four substitutions of Asn51-Ile and Cys59-Arg as well as active site residues Ser108-Asn and Ile164-Leu (Figure 1C). The spread of resistance in parasites halted further development of antifolate antimalarials, with Pyr being combined with sulfadoxine in the 1960s to boost the efficacy of pyrimethamine.

The elucidation of the *Pf*DHFR WT and QM crystal structures allowed for a renaissance of antifolate antimalarials [10]. Utilising X-ray crystallography in addition to mutagenesis techniques, the resistance mechanisms within the active site were identified and explored [22–24]. First generation antifolates (Figure 1B,E) have a *para*-chlorophenyl moiety that fits into the active site when Ser108 is present. *Pf*DHFR QM has a mutation of Ser108 to Asn108, which causes a steric clash between enzyme and inhibitor, resulting in poor binding. Inhibitors that replaced the rigid aryl group with a flexible chain avoided steric clashes with position 108 and showed greater affinity for both WT and QM *Pf*DHFR by interacting with residues further away in the active site [25,26]. A study of Pyr-resistant *Pf*DHFR obtained from field isolates found that no strain had a mutation at Asp54, implying that this residue may be essential for enzyme activity [25]. Further investigations revealed that mutation of Asp54 to any amino acid except Glu, resulted in complete loss of enzymatic activity, indicating that the carboxyl group of Asp54 is required for enzymatic function [24]. The identification of Asp54 as an essential active site residue enables *Pf*DHFR inhibitors to be designed with Asp54 acting as an anchor point.

More recently, development of antifolates (Figure 1E) have had a heavy focus on designing inhibitors to be effective in both Pyr-resistant and Pyr-sensitive strains of *Pf*. These campaigns utilise information obtained from the X-ray crystal structures and molecular dynamics to inform the inhibitor design. One of the earliest modern inhibitors was **WR99210** (**3**), which was potent against both WT and QM *Pf*DHFR. **WR99210** featured a 2,4-diaminodihydrotriazine ring, which anchored the molecule to Asp54. The inhibitory activity of **WR99210** against both WT and QM *Pf*DHFR was due to the inclusion of a flexible 5-membered chain, which bridged the dihydrotriazine ring to a 2,4,5-trichlorophenyl moiety. The flexible linker provided the trichlorophenyl ring with access to a region deeper within the active site, whilst avoiding residue 108. However, **WR99210** suffered from gastrointestinal tract toxicity and poor oral bioavailability, caused by basicity of the dihydrotriazine [27,28]. Saepua et al. [29] reported a range of pyrimethamine derivatives active against both WT and QM *Pf*DHFR, including potent analogue **4**. These compounds possess a similar pharmacophore to **WR99210**, with the pyrimidine heterocycle interacting strongly with Asp54. The 4-atom linker of **4** extends a *meta*-phenoxyacetic acid group further into the active site, allowing for hydrophobic interactions between
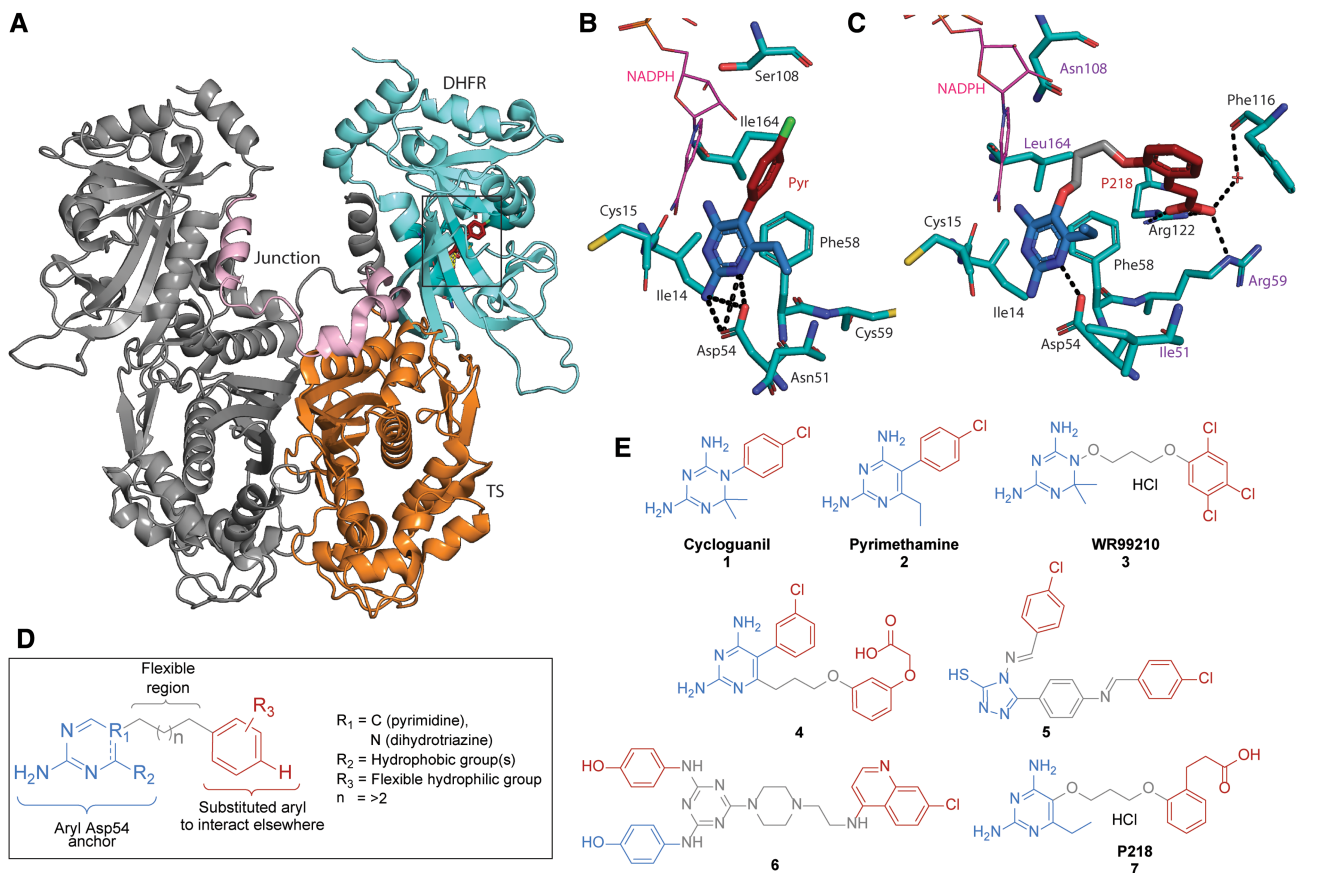
Figure 1. PfDHFR and inhibitors.

(**A**) Cartoon model of the X-ray structure of WT PfDHFR-TS dimer bound to Pyr, where one monomer is shown with DHFR domain in cyan, TS domain in orange and junction region in pink. The dimer partner is shown in grey. (PDB ID 3QGT) (**B**) Zoom of Pyr (in sticks with red/blue carbon atoms) bound to wild-type PfDHFR (in sticks and carbon atoms in aqua) and NADPH (in lines, carbon atoms magenta). Hydrogen bonds indicated by black dashed lines. (PDB ID 3QGT) (**C**) Binding conformation of **P218** (blue/grey/red sticks) with quadruple mutant PfDHFR (aqua sticks) and NADPH (in lines, carbon atoms magenta), with hydrogen bonds indicated by dashed lines. Mutant residues are indicated with violet labels. (PDB ID 4DP3) (**D**) Pharmacophore of potent PfDHFR inhibitors. Effective inhibitors typically feature a nitrogenous heterocycle (blue) that interacts with Asp54 and a substituted aromatic ring (red) which has the ability to form hydrogen bonds with residues conserved between WT and QM PfDHFR. These two binding groups are linked by a flexible region (grey) at least 4-atoms long and can be hydrophobic or hydrophilic. (**E**) 2D structures of PfDHFR inhibitors, Asp54 binding motif in blue, linker region in grey and secondary binding motif in red.

Phe58, Phe116 and the phenyl ring. The carboxylate moiety of the phenoxyacetic acid forms charge-mediated hydrogen-bonds with Arg59 and an additional interaction with Arg122 via an intermediary water molecule [29]. Other PfDHFR inhibitory studies feature chemical classes other than dihydrotriazines and pyrimidines, however, still maintain the Asp54 interaction. Thakkar et al. reported a series of triazoles (e.g. **5**) that displayed potent inhibitory activity against WT PfDHFR. The thiol interacts with Asp54, whilst being supported by additional π interactions between the triazole and active site. The two para-chlorophenyl groups extend into different regions of the active site to form various hydrophobic interactions [30]. Bhat et al. reported a series of 4-aminoquinoline-triazine bifunctional hybrids that showed moderate activity against chloroquine-sensitive (3D-7) and chloroquine-resistant (RKL-2) Pf. These compounds target DHFR with the triazine moiety, whilst the quinolone group is able to inhibit the conversion of haem to haemozoin. In DHFR, one of the phenols of **6** anchors the molecule to Asp54 as well as forming π–π interactions with adjacent Phe58 [31].

The current clinical candidate **P218** (**7**), is a potent inhibitor of both WT and QM PfDHFR that is under development by MMV in partnership with Janssen and recently proved to have a good safety profile in healthy human volunteers [21]. **P218** is based on a 2,4-diaminopyrimidine scaffold (**7**, blue) and a 3-phenylpropanoic

moiety (**7**, red) connected by a 5-atom linker (**7**, grey) [28]. The selection of the pyrimidine was based on previously reported mechanistic information, acting as the Asp54 anchor. Furthermore, pyrimidine was chosen over dihydrotriazine due to the superior oral bioavailability of pyrimidines and the toxicity associated with dihydrotriazines [27,28]. Co-crystal structures of **P218** bound to WT and QM (Figure 1C) *Pf*DHFR revealed that the 5-atom linker steers the 3-phenylpropanoic acid group away from residue 108. The carboxylate of the 3-phenylpropanoic acid moiety forms charge-mediated hydrogen bonds with Arg122 and Arg59. Arg122 is conserved across QM and WT *Pf*DHFR, with the aliphatic portion of the side chain highly restrained by surrounding residues [28]. This restrained side-chain serves as a rigid and reliable platform for ionic interactions to be formed. The replacement of *Pf*DHFR Met55, Cys/Arg59 and Phe116 with structurally equivalent human DHFR Phe31, Gln35 and Asn64 resulted in the Arg side-chain restriction not being observed in human DHFR, which caused **P218** to adopt a radically different conformation in human DHFR and does not form interactions with equivalent Arg70, providing necessary selectivity to the **P218** [28,32]. The carefully considered design of **P218** resulted a highly potent inhibitor of QM *Pf*DHFR ($K_i = 0.54 \pm 0.12$ nM), which displays good antiplasmodial activity against both WT and QM *Pf* ($IC_{50} = 4.6 \pm 1.6$ and 56 ± 20 nM, respectively) [28], and possesses a favourable safety and tolerability profile [21]. Target-based drug design has played a crucial role in the discovery and development of this promising clinical candidate.

*Pf*DHODH — Structural data providing a route to selective inhibition

Plasmodium parasites rely entirely on the *de novo* biosynthesis pathway for their pyrimidine, an essential metabolite precursor for DNA and RNA synthesis [33–36]. Inhibition of pyrimidine biosynthesis results in parasite death in both the blood and liver stages, making the pathway an attractive target for drug development [37]. Dihydroorotate dehydrogenase is involved in the fourth step of the pyrimidine pathway and utilises flavin mononucleotide (FMN) and coenzyme Q (CoQ) to catalyse the oxidation of dihydroorotate (DHO) to orotate (ORO) [38]. DHODH enzymes exist as either cytosolic enzymes (class I) or membrane-associated (class II) [39,40]. *Plasmodium* DHODH are class II enzymes that form a conserved catalytic α/β-barrel (Figure 2A), composed of eight-strand β-barrel (in cyan) wrapped by eight α-helices (in tan), as well as a highly sequence variable hydrophobic N-terminal extension (in grey) [39,41]. This N-terminal extension forms a domain of two α-helices, located close to the top of the barrel and a tunnel-like pocket is formed as a result of the packing [41]. The active site of the enzyme is located within the barrel and contains the binding sites for FMN (Figure 2A, shown in yellow) [39]. Inhibitors of the enzymes can bind directly in the barrel blocking substrate access [41,42] or within the tunnel-like pocket near the N-terminal extension blocking the electron transfer between FMN and CoQ [41,43]. Targeting inhibitors to the tunnel binding site provides a route to selective enzyme inhibitors due to high sequence variability and conformational mobility of this region [41]. The tunnel binding site has three regions, a hydrophilic pocket comprising highly conserved residues His185 and Arg265; a hydrophobic pocket that contains key aromatics Phe188 and Phe227 involved in inhibitor positioning and finally a small hydrophobic channel leading toward FMN lined by Val532, Ile272 and Ile263 (Figure 2B–D) [41,44].

Development of potent *Plasmodium*-specific inhibitors was challenging prior to the resolution of the *Pf*DHODH structure [45–47]. The first X-ray crystal structure of *Pf*DHODH was solved bound to a human *Hs*DHODH inhibitor (**A77-1726**) (Figure 2B) [41]. **A77-1726** binds to the species-selective inhibitor site in both enzymes and is a potent inhibitor of *Hs*DHODH but only a moderate inhibitor of *Pf*DHODH ($IC_{50} = 0.261$ and 190 μM, respectively) [43,44,48]. In *Hs*DHODH, the trifluoromethylphenyl moiety of **A77-1726** sits in the large hydrophobic pocket, and the polar carbonyl, nitrile and enol groups hydrogen-bond to Arg136, Tyr356, His56 and Gln47, respectively [41,49]. The species-selective inhibitor site in *Pf*DHODH is significantly smaller than the human enzyme due to the presence of sequence changes, namely Met536, Phe174 and Phe188 that close the tunnel from different sides and substitutions of two Val residues with Ile at the end of the tunnel (Figure 2B) [41]. In *Pf*DHODH, the orientation of Phe188 pushes the trifluoromethylphenyl moiety closer to the first helix resulting in an almost 180° rotation of **A77-1726** about its long axis (Figure 2B, *Pf*-**A77-1726** in blue and *Hs*-**A77-1726** in red). This shift disrupts hydrogen-bonding that likely contributes to potency observed toward *Hs*DHODH. The conserved His185 and Arg265 (Figure 2B in orange) hydrogen bond with the carbonyl and enol groups of **A77-1726** in *Pf*DHODH as opposed to the long-distance water-mediated contacts in *Hs*DHODH [41]. The variation in the binding tunnels of the two enzymes suggests that ligand binding in *Pf*DHODH is directed by hydrophobic interactions, notably stacking interactions with Phe188 and Phe227
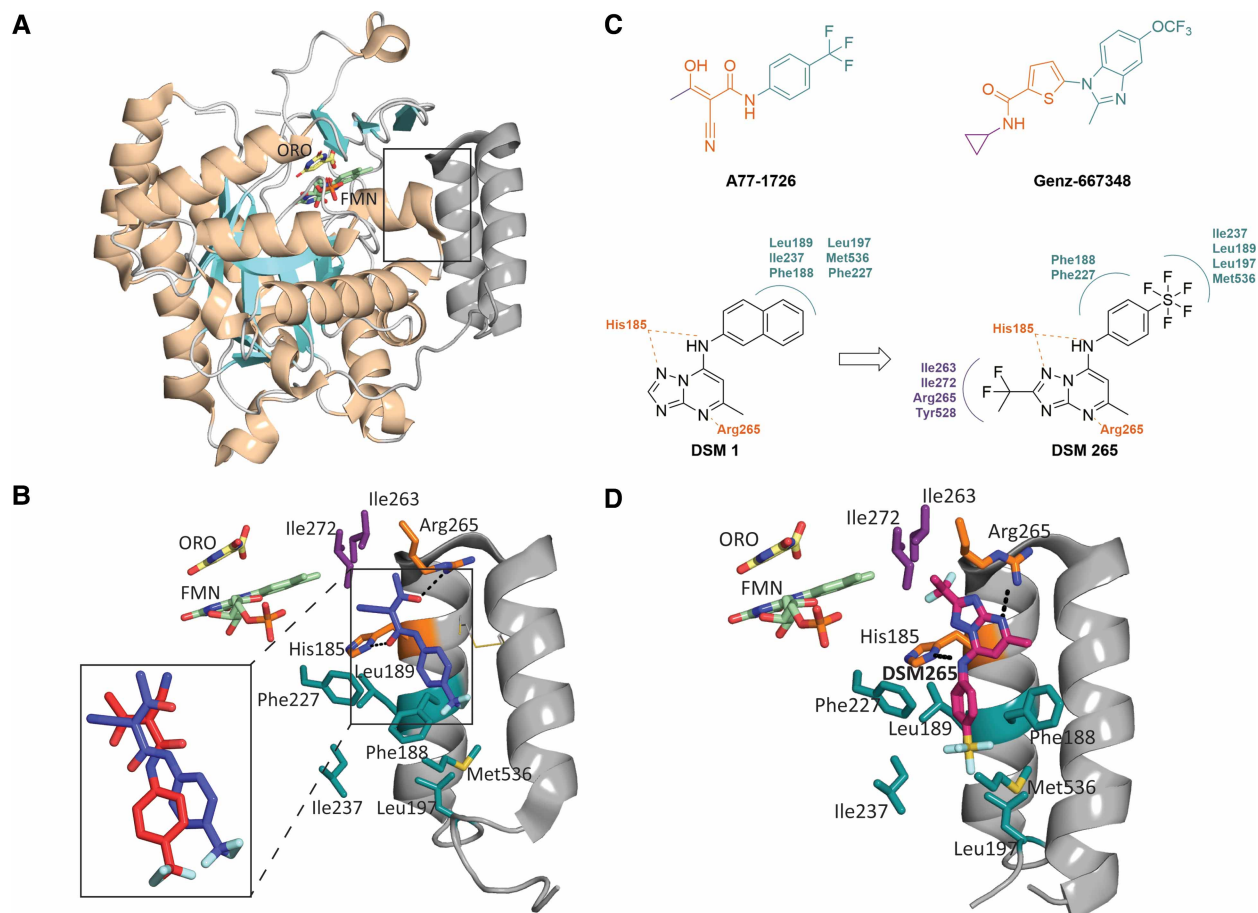
Figure 2. *Pf*DHODH and inhibitors.
(**A**) The X-ray structure of *Pf*DHODH (PDB ID 1TV5) demonstrating the central α/β-barrel (α-helices in tan, β-barrel in cyan) and the two α-helices of the N-terminal domain in grey. Substrates FMN and ORO are shown in stick with green and yellow carbons, respectively. The species-specific site of inhibitor binding is indicated by the box in black. (**B**) The inhibitor binding site from the co-crystal structure of *Pf*DHODH and **A77-1726** (PDB ID 1TV5), *Pf*-**A77-1726** is shown in blue sticks, residue sidechains are shown in sticks, hydrophobic pocket in teal, hydrophilic pocket in orange and small hydrophobic tunnel in purple. In the black box the structures of *Hs*-**A77-1726** and *Pf*-**A77-1726** are overlayed to demonstrate the different binding orientations; **A77-17266** is shown in sticks with *Pf* in blue carbons and *Hs* in red carbons. (**C**) 2D chemical structure of inhibitors discussed; hydrophobic region in teal, hydrophilic region in orange and small hydrophobic channel in purple. Also showing the hit-lead evolution starting with **DSM1** to get to **DSM265**, the clinical candidate and the residues involved in binding. (**D**) The inhibitor binding site from the co-crystal structure of **DSM265** bound to *Pf*DHODH (PDB ID 4RX0) coloured as per B with **DSM265** in magenta and hydrogen-bonds indicated by black dashes.

(Figure 2B in teal), while the conserved residues form important hydrogen-bonds [41]. The methyl group of **A77-1726** extends toward the small, hydrophobic cavity (in purple) [48].

Subsequent studies investigated derivatives of **A77-1726** and other scaffolds with alternating hydrophilic head and hydrophobic tail groups, as well as exploring the small hydrophobic cavity but resulted in a series with only mid- to sub-micromolar activity [48,50–55]. Target-based HTS campaigns identified a thiophene-carboxamide as a new starting block for *Pf*DHODH inhibitors [52]. Structure-based drug design of the initial thiophene-carboxamide hit delivered **Genz-667348** (PDB ID 3O8A) that showed selective, low nanomolar activity toward *Pf*DHODH [56,57]. The benzimidazole of **Genz-667348** sits in the hydrophobic pocket forming edge-to-face stacking interactions with Phe188 (Figure 2C in teal), while N and O atoms of the amide moiety sit in the hydrophilic pocket and form hydrogen-bonds with His185 and Arg265, respectively (in orange) [56]. The cyclopropyl group of **Genz-667348** occupies the narrow hydrophobic channel (in purple), and an increase in the ring size resulted in a loss of activity [56–58]. Despite promising pan-parasitic target inhibition *in vitro*, efficacy *in vivo* and acceptable ADME/PK, these inhibitors have not advanced beyond late lead development stage [56–59].

The compound **DSM1** was also identified from a target-based HTS (Figure 2C) [47,60]. Early structural studies showed that the triazolopyrimidine moiety sat in the hydrophilic pocket (Figure 2C in orange) and the naphthyl group occupied hydrophobic pocket (in teal) [44]. Within the hydrophilic pocket, the bridging nitrogen $N-1$ in the triazolopyrimidine inhibitors is able to delocalise electrons into the ring, establishing dipoles in the inhibitor that permit hydrogen-bonds between the bridging nitrogen $N-1$ and His185, as well as the pyridine nitrogen $N-5$ and Arg265 (shown in orange). This was identified as a key factor in the potency of this inhibitor class and replacement of $N-1$ atom in **DSM1** with either O or S results in complete loss of activity as these atoms are unable to induce this delocalisation effect [44,61]. In the hydrophobic pocket, the position of the naphthyl group shifted Phe188 to allow for edge-to-face stacking (in teal), and thus extending **DSM1** further than the trifluoromethylphenyl of **A77-1726**. Subsequent structure-based design investigated replacing the naphthyl group in **DSM1** with substituted phenyls and showed that the hydrophobic pocket prefers bulky *para*-substituted phenyl groups where 4-SF_5-Ph (as demonstrated by **DSM265**) represents the best balance between desirable potency, metabolic stability and plasma exposure [44,60]. Additionally, it was found that *ortho*- or *meta*-substituents resulted in a loss of activity likely due to the lack of space within the pocket [44]. Replacement of 4-SF_5-Ph with CF_3-pyridinyls in the hydrophobic pocket improved drug-like properties [62], however, unexpected off-target toxicity later halted the progress of this analogue [63].

DSM1 and the bound crystal structure allowed rapid progress to identify more potent compounds with desirable physicochemical properties. The C-5 atom of **DSM1** provided a route into the narrow hydrophobic tunnel, and subsequent exploration identified that small substitutions at the C-5 position pick up additional hydrophobic interactions available in this cavity [44,64]. **DSM265** is the outcome of this successful program and possesses desirable potency, *in vivo* efficacy, long half-life and excellent oral exposure [64]. It binds *Pf*DHODH with triazolopyrimidine moiety occupying the hydrophilic pocket (in orange), the CF_2CH_3 substitution sitting in the hydrophobic channel (in purple) while the main hydrophobic pocket encapsulates the 4-SF_5-Ph group (in teal) (Figure 2C,D) [37,64]. **DSM265** is currently being developed by MMV in partnership with Takeda and has shown promise in Phase Ia/b studies as a single-dose treatment and as a once-weekly chemoprophylaxis as well as Phase IIa efficacy studies in patients with *Pf* and *Pv* malaria infections [65–68]. **DSM265** has completed Phase IIa clinical trials and a number of other *Pf*DHODH inhibitors have also been designed and synthesised utilising the understanding of target mechanism [59,69–73]. Altogether, these efforts have not only validated *Pf*DHODH as a clinical target but have resulted in desirable clinical candidates.

*Pf*A-M1 — Flexible substrate pockets provide key to potency

The *Pf* M1 aminopeptidase (*Pf*A-M1) is a clan MA zinc-dependent metalloaminopeptidase (MAP) which has been a potential antimalarial target of interest for over a decade [74–76]. *Pf*A-M1 is involved in the terminal stages of haemoglobin digestion by facilitating the final stages of haemoglobin peptide hydrolysis into single amino acids [77–79]. Haemoglobin digestion is a semi-ordered enzymatic cascade that is essential for parasite proliferation. *Plasmodium* spp are unable to synthesise amino acids, so rely on this process heavily during the trophozoite and schizont phases of the intra-erythrocytic life-cycle. These phases require an abundance of amino acids to ensure sufficient parasite growth and to prevent premature haemolysis [80]. *Pf*A-M1 is an essential enzyme [74] and is highly expressed throughout the parasite cytosol and digestive vacuole [81].

In *Pf*, *Pf*A-M1 remains inactive until a 196 residue extended N-terminus is hydrolysed and the enzyme is released [82]. The X-ray crystal structure of the soluble, active enzyme has been extensively studied, with the tertiary structure being divided into four domains, consisting of 26 α-helices and seven β-sheets arranged in a bacterial aminopeptidase N-fold (Figure 3A) [81]. *Pf*A-M1 possesses the two signature M1 aminopeptidase family motifs, the zinc-binding and substrate coordination motifs [74]. The substrate pool of *Pf*A-M1 has also been investigated, with a broad specificity for bulky, hydrophobic and basic P1 residues being observed [83]. Early work to identify the effects generated by the inhibition of *Pf*A-M1 was conducted using compounds from a bestatin-based library [79]. Selective inhibition of *Pf*A-M1 *in vitro* resulted in a distinctive digestive vacuole swelling [79]. The change in vacuole morphology was dose-dependent and hypothesised to be caused by an excess of oligopeptides, which are too large to be exported to the cytosol. The outcomes of selective *Pf*A-M1 inhibition *in vivo* have not yet been determined, however, studies using inhibitors that can target both *Pf*A-M1 as well as the M17 aminopeptidase have shown that inhibition of these two enzymes can control parasite growth in murine models [84,85].
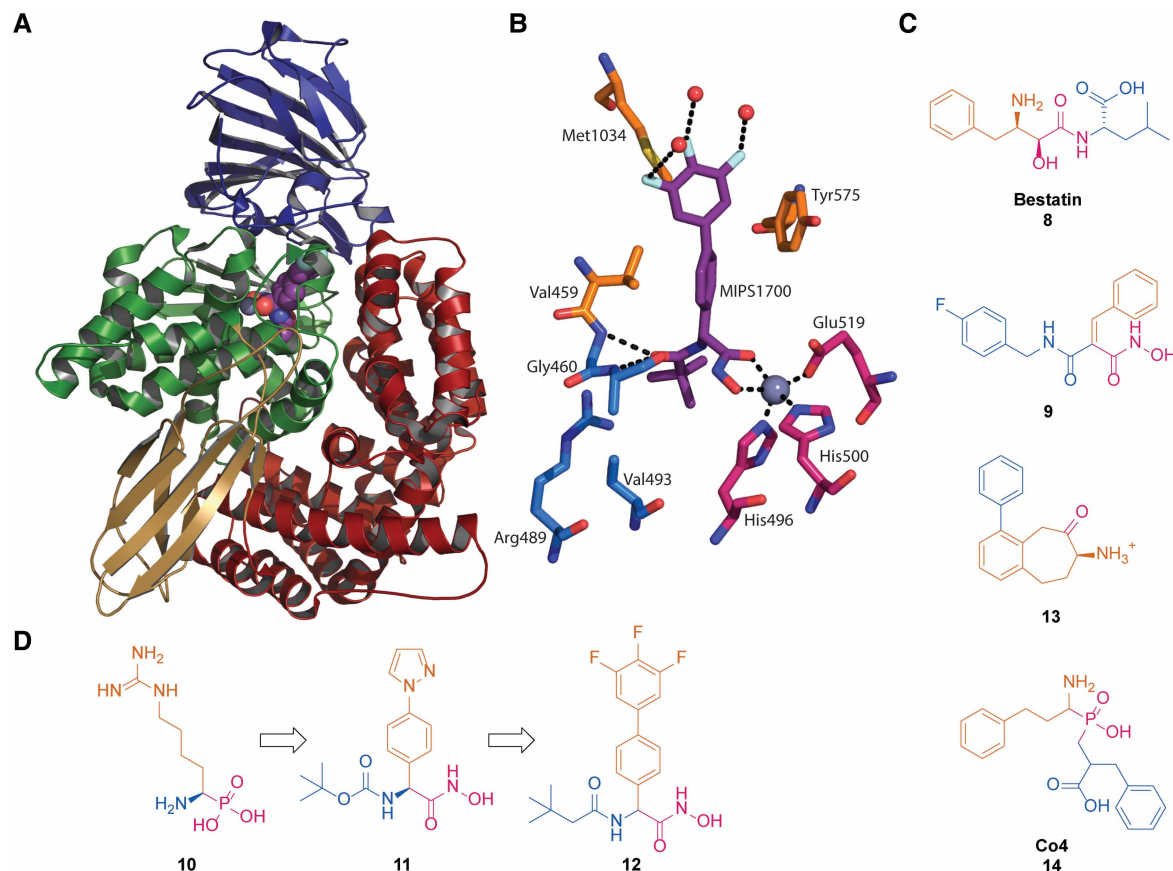
Figure 3. *Pf*A-M1 and inhibitors.

(**A**) The X-ray structure of *Pf*A-M1 (PDB ID 4ZX4) demonstrating four domains in yellow, green, red and dark blue. (**B**) A closeup of the co-crystal structure of *Pf*A-M1 and **MIPS1700** (**12**) showing the inhibitor binding site with the important amino acids involved in forming interactions; **MIPS1700** in purple, S1 pocket in orange, S1′ pocket in blue, ZBG and catalytic triad in pink. (**C**) A number of inhibitors reported in literature; colour-coded per respective region. (**D**) The chemical evolution starting with the arginine mimetic (**10**) and ending with the most recent published inhibitor (**12**).

*Pf*A-M1 is a zinc-dependent enzyme and to date, all inhibitors produced have targeted the essential Zn^{2+} in the active site. The binding pose of the inhibitors is largely determined by the zinc binding group (ZBG) coordination. The co-crystal structure of the early inhibitors show that the Zn^{2+} itself is co-ordinated to the enzyme by a catalytic triad of residues His496, His500, and Glu519 while the ZBG of the inhibitor is co-ordinated to the Zn^{2+} through metallo-bonds (Figure 3B, in pink) [74]. For instance, bestatin (Figure 3C, **8**) [79] utilises its hydroxyl and carbonyl oxygen while other peptide-based inhibitors [85–87] utilise their carboxylic acid moiety for coordination. Other studies explored the use of phosphonic acids and aminophosphonates (e.g. **10** and **14**) [88–91] and while they exhibited excellent ZBG properties for coordination, these moieties often suffer from permeability issues and were produced largely as tool compounds. As a result, more recent compounds utilise groups like hydroxamic acids (**9**, **11**, and **12**, this type of coordination is demonstrated in Figure 3B) [90–95] and geminal-diol (**13**) [96–98] for the coordination of Zn^{2+}. Although targeting the Zn^{2+} is essential, the approach raises challenges for selectivity of the parasite target over human homologues — parasite specific inhibitors therefore require the employment of specific interactions with the *Pf*A-M1 S1 and S1′ subsites [81].

The SAR of the S1 and S1′ pockets of *Pf*A-M1 have been thoroughly explored within various campaigns. The S1 pocket (Figure 3B) is made up of several hydrophobic residues as well as Glu572, a flexible and polar residue in the pocket that permits conformational changes upon ligand binding to allow for larger side chains in this pocket [74,86,99]. In 2006, Flipo et al. [91] reported a series of malonyl-hydroxamic acids, similar to **9**, probing

the active site. Although the importance of metal chelation was understood, the lack of crystal structures at this stage made the efficient design of potent inhibitors challenging. To develop the understanding of the binding mode and the subsite SAR, a study by Deprez-Poulain et al. [100] utilised the *Pf*A-M1 crystal structure in conjunction with docking studies to identify the key interactions formed in the S1 and S1′ pockets. Furthermore, Sivaraman et al. studied a small library of phosphonic acid arginine mimetics. The biaryl pyrazole-phenyl scaffold (**11**) was found to outperform the arginine moiety (**10**), caused by hydrophobic interactions between pyrazole and Met1034 [89]. Further SAR studies by the same group, showed improved interactions with fluoro-substituted biphenyl ring systems (**12**) [94,95]. X-ray crystal structures demonstrate that this system allows the 3,4,5-trifluorophenyl ring to sit deeper in the S1 pocket and enter an intricate network of water-mediated hydrogen-bonds (Figure 3B, shown in orange). More recently, a series of aminobenzosuberone inhibitors (e.g. **13**) with selective *Pf*A-M1 inhibition over other MAPs were reported [96–98].

The S1′ pocket consists of predominantly hydrophobic residues, however, it also allows for some hydrophilic interactions (Figure 3B) [74,95]. Early studies involving bestatin derivatives indicated that the S1′ pocket favours smaller aliphatic side chains [86,89]. SAR studies of different inhibitors probing this pocket and the comparison of their crystal structures indicate that the spatial differences in the S1′ cavity is the major contributor to the enzyme selectivity of *Pf*A-M1 over other MAPs (*Pf*A-M17) [94,95]. Computational studies have shown that measurements of pocket size from crystal structures are influenced by crystal packing [101]. These two facts highlight some of the challenges of compound design and the strong need to consider mechanism and how the target responds to inhibition. The development of these *Pf*A-M1 inhibitors has relied heavily on target-based drug design. Combining *in silico* and structure-based drug development principles has allowed for the efficient design, synthesis and biological evaluation of potent cross-species dual-inhibitors. The design of future *Pf*A-M1 inhibitors should exploit existing structural data, with focus on forming interactions deep within the S1′ region. This site has usually been regarded as a hydrophobic pocket, however, compounds that target hydrophilic residues such as Arg489 and Thr577 have largely been unexplored. To advance potent inhibitors with desirable drug-like properties, these structural changes should be made while taking PK and ADME properties into consideration.

Perspectives

- **Importance of the field:** Malaria remains a global health burden and the emergence of resistance reduces the effectiveness of current treatment options, prompting an urgency for the discovery of novel antimalarial agents.

- **Summary of current thinking:** Target-based drug design relies on understanding of target mechanism, and takes advantage of available knowledge of the structural and functional data to inform the design of candidates while also overcoming challenges associated with the targets. *Pf*DHFR, *Pf*DHODH, *Pf*A-M1 and their inhibitors highlight how this process can be used to design potent inhibitors.

- **Future directions:** With the advances in antiparasitic target-identification and recent developments of techniques such as cryo-electron microscopy, structure-based drug design is positioned to be far more prominent in future antimalarial campaigns.

Competing Interests

The authors declare that there are no competing interests associated with the manuscript.

PORTLAND
PRESS

Acknowledgements

Author Contributions

P.P.S.C. and M.M. contributed equally. All authors contributed to concept and writing of manuscript. All authors declare they have no conflict of interest.

Abbreviations

ACT, artemisinin combination therapy; ADME, absorption, distribution, metabolism and excretion; CoQ, coenzyme Q; DHFR, dihydrofolate reductase; DHO, dihydroorotate, DHODH, dihydroorotate dehydrogenase; FMN, flavin mononucleotide; HTS, high-throughput screen; MAP, metalloaminopeptidase; MMV, medicines for malaria venture; MoA, mechanism of action; NADPH, nicotinamide adenine dinucleotide phosphate; nM, nanomolar; ORO, orotate; PDB, protein data bank; *Pf*, *Plasmodium falciparum*; *Pf*A-M1, *P. falciparum* M1 aminopeptidase; PK, pharmacokinetics; *Pv*, *Plasmodium vivax*; Pyr, pyrimethamine; QM, quadruple mutant; SAR, structure-activity relationship; TS, thymidylate synthase; WHO, World Health Organisation; WT, wild-type; ZBG, zinc-binding group.

References

1 WHO. (2019) *World Malaria Report 2019*, World Health Organization, Geneva
2 WHO. (2015) *Global Technical Strategy for Malaria 2016–2030*, World Health Organization, Geneva
3 Dondorp, A., Yeung, S., White, L., Nguon, C., Day, N., Socheat, D. et al. (2010) Artemisinin resistance: current status and scenarios for containment. *Nat. Rev. Microbiol.* **8**, 272–280 https://doi.org/10.1038/nrmicro2331
4 O'Brien, C., Henrich, P.P., Passi, N. and Fidock, D.A. (2011) Recent clinical and molecular insights into emerging artemisinin resistance in *Plasmodium falciparum. Curr. Opin. Infect. Dis.* **24**, 570–577 https://doi.org/10.1097/QCO.0b013e32834cd3ed
5 Gilbert, I.H., Leroy, D.A. and Frearson, J. (2011) Finding new hits in neglected disease projects: target or phenotypic based screening? *Curr. Top. Med. Chem.* **11**, 1284–1291 https://doi.org/10.2174/156802611795429176
6 Swinney, D.C. (2013) Phenotypic vs. target-based drug discovery for first-in-class medicines. *Clin. Pharmacol. Ther.* **93**, 299 https://doi.org/10.1038/clpt.2012.236
7 Sykes, M.L. and Avery, V.M. (2013) Approaches to protozoan drug discovery: phenotypic screening. *J. Med. Chem.* **56**, 7727–7740 https://doi.org/10.1021/jm4004279
8 Chen, M.J., Shimada, T., Moulton, A.D., Cline, A., Humphries, R.K., Maizel, J. et al. (1984) The functional human dihydrofolate reductase gene. *J. Biol. Chem.* **259**, 3933–3943 PMID:6323448
9 Ivanetich, K.M. and Santi, D.V. (1990) Bifunctional thymidylate synthase-dihydrofolate reductase in protozoa. *FASEB J.* **4**, 1591–1597 https://doi.org/10.1096/fasebj.4.6.2180768
10 Yuvaniyama, J., Chitnumsub, P., Kamchonwongpaisan, S., Vanichtanankul, J., Sirawaraporn, W., Taylor, P. et al. (2003) Insights into antifolate resistance from malarial DHFR-TS structures. *Nat. Struct. Mol. Biol.* **10**, 357–365 https://doi.org/10.1038/nsb921
11 Nzila, A. (2006) The past, present and future of antifolates in the treatment of *Plasmodium falciparum* infection. *J. Antimicrob. Chemother.* **57**, 1043–1054 https://doi.org/10.1093/jac/dkl104
12 Greenwood, D. (1995) Conflicts of interest: the genesis of synthetic antimalarial agents in peace and War. *J. Antimicrob. Chemother.* **36**, 857 https://doi.org/10.1093/jac/36.5.857
13 Smith, C.L. and Powell, K.R. (2000) Review of the sulfonamides and trimethoprim. *Pediatr. Rev.* **21**, 368–371 https://doi.org/10.1542/pir.21-11-368
14 Masters, P.A., O'Bryan, T.A., Zurlo, J., Miller, D.Q. and Joshi, N. (2003) Trimethoprim-sulfamethoxazole revisited. *Arch. Intern. Med.* **163**, 402–410 https://doi.org/10.1001/archinte.163.4.402
15 Farber, S., Diamond, L.K., Mercer, R.D., Sylvester, R.F. and Wolff, J.A. (1948) Temporary remissions in acute leukemia in children produced by folic acid antagonist, 4-aminopteroyl-glutamic acid (Aminopterin). *N. Engl. J. Med.* **238**, 787–793 https://doi.org/10.1056/NEJM194806032382301
16 Gregson, A. and Plowe, C. (2005) Mechanisms of resistance of malaria parasites to antifolates. *Pharmacol. Rev.* **57**, 117–145 https://doi.org/10.1124/pr.57.1.4
17 Ashton, T.D., Devine, S.M., Möhrle, J.J., Laleu, B., Burrows, J.N., Charman, S.A. et al. (2019) The development process for discovery and clinical advancement of modern antimalarials. *J. Med. Chem.* **62**, 10526 https://doi.org/10.1021/acs.jmedchem.9b00761
18 Gatton, M.L., Martin, L.B. and Cheng, Q. (2004) Evolution of resistance to sulfadoxine-pyrimethamine in *Plasmodium falciparum. Antimicrob. Agents. Chemother.* **48**, 2116 https://doi.org/10.1128/AAC.48.6.2116-2123.2004
19 Cowman, A.F., Morry, M.J., Biggs, B.A. and Foote, S.J. (1988) Amino acid changes linked to pyrimethamine resistance in the dihydrofolate reductase-thymidylate synthase gene of *Plasmodium falciparum. Proc. Natl Acad. Sci. U.S.A.* **85**, 9109–9113 https://doi.org/10.1073/pnas.85.23.9109
20 Basco, L.K., Tahar, R. and Ringwald, P. (1998) Molecular basis in vivo resistance to sulfadoxine-pyrimethamine in African adult patients infected with *Plasmodium falciparum. Parasitol. Int.* **42**, 117–117 https://doi.org/10.1016/S1383-5769(98)80253-5
21 Chughlay, M.F., Rossignol, E., Donini, C., El Gaaloul, M., Lorch, U., Coates, S. et al. (2020) First-in-human clinical trial to assess the safety, tolerability and pharmacokinetics of P218, a novel candidate for malaria chemoprotection. *Br. J. Clin. Pharmacol.* **86**, 1113–1124 https://doi.org/10.1111/bcp.14219

22   Peterson, D.S., Walliker, D. and Wellems, T.E. (1988) Evidence that a point mutation in dihydrofolate reductase-thymidylate synthase confers resistance to pyrimethamine in falciparum malaria. *Proc. Natl Acad. Sci. U.S.A.* **85**, 9114–9118 https://doi.org/10.1073/pnas.85.23.9114

23   Ferlan, J.T., Mookherjee, S., Okezie, I.N., Fulgence, L. and Sibley, C.H. (2001) Mutagenesis of dihydrofolate reductase from *Plasmodium falciparum*: analysis in *Saccharomyces cerevisiae* of triple mutant alleles resistant to pyrimethamine or WR99210. *Mol. Biochem. Parasitol.* **113**, 139–150 https://doi.org/10.1016/S0166-6851(01)00207-9

24   Sirawaraporn, W., Sirawaraporn, R., Yongkiettrakul, S., Anuwatwora, A., Rastelli, G., Kamchonwongpaisan, S. et al. (2002) Mutational analysis of *Plasmodium falciparum* dihydrofolate reductase: the role of aspartate 54 and phenylalanine 223 on catalytic activity and antifolate binding. *Mol. Biochem. Parasitol.* **121**, 185–193 https://doi.org/10.1016/S0166-6851(02)00035-X

25   Yuthavong, Y., Yuvaniyama, J., Chitnumsub, P., Vanichtanankul, J., Chusacultanachai, S., Tarnchompoo, B. et al. (2005) Malarial (*Plasmodium falciparum*) dihydrofolate reductase-thymidylate synthase: structural basis for antifolate resistance and development of effective inhibitors. *Parasitology* **130**, 249–259 https://doi.org/10.1017/S003118200400664X

26   Tarnchompoo, B., Sirichaiwat, C., Phupong, W., Intaraudom, C., Sirawaraporn, W., Kamchonwongpaison, S. et al. (2002) Development of 2,4-diaminopyrimidines as antimalarials based on inhibition of the S108N and C59R + S108N mutants of dihydrofolate reductase from pyrimethamine-resistant *Plasmodium falciparum*. *J. Med. Chem.* **45**, 1244–1252 https://doi.org/10.1021/jm010131q

27   Rieckmann, K., Yeo, A. and Edstein, M.D. (1996) Activity of PS-15 and its metabolite, WR99210, against *Plasmodium falciparum* in an in vivo-in vitro model. *Trans. Roy. Soc. Trop. Med. Hyg.* **90**, 568–571 https://doi.org/10.1016/S0035-9203(96)90326-0

28   Yuthavong, Y., Tarnchompoo, B., Vilaivan, T., Chitnumsub, P., Kamchonwongpaisan, S., Charman, S.A. et al. (2012) Malarial dihydrofolate reductase as a paradigm for drug development against a resistance-compromised target. *Proc. Natl Acad. Sci. U.S.A.* **109**, 16823 https://doi.org/10.1073/pnas.1204556109

29   Saepua, S., Sadorn, K., Vanichtanankul, J., Anukunwithaya, T., Rattanajak, R., Vitsupakorn, D. et al. (2019) 6-Hydrophobic aromatic substituent pyrimethamine analogues as potential antimalarials for pyrimethamine-resistant *Plasmodium falciparum*. *Bioorg. Med. Chem.* **27**. https://doi.org/10.1016/j.bmc.2019.115158

30   Thakkar, S.S., Thakor, P., Doshi, H. and Ray, A. (2017) 1,2,4-triazole and 1,3,4-oxadiazole analogues: synthesis, MO studies, in silico molecular docking studies, antimalarial as dhfr inhibitor and antimicrobial activities. *Bioorg. Med. Chem.* **25**, 4064–4075 https://doi.org/10.1016/j.bmc.2017.05.054

31   Bhat, H.R., Singh, U.P., Gahtori, P., Ghosh, S.K., Gogoi, K., Prakash, A. et al. (2013) 4-aminoquinoline-1,3,5-triazine: design, synthesis, in vitro antimalarial activity and docking studies. *New J. Chem.* **37**, 2654–2662 https://doi.org/0.1039/c3nj00317e

32   Abbat, S., Jain, V. and Bharatam, P.V. (2015) Origins of the specificity of inhibitor P218 toward wild-type and mutant Pfdhfr: a molecular dynamics analysis. *J. Biomol. Struct. Dyn.* **33**, 1913–1928 https://doi.org/10.1080/07391102.2014.979231

33   Krungkrai, J. (1995) Purification, characterization and localization of mitochondrial dihydroorotate dehydrogenase in *Plasmodium falciparum*, human malaria parasite. *Biochim. Biophys. Acta. Gen. Subj.* **1243**, 351–360 https://doi.org/10.1016/0304-4165(94)00158-T

34   Hyde, J.E. (2007) Targeting purine and pyrimidine metabolism in human apicomplexan parasites. *Curr. Drug Targets* **8**, 31–47 https://doi.org/10.2174/138945007779315524

35   Gardner, M.J., Hall, N., Fung, E., White, O., Berriman, M., Hyman, R.W. et al. (2002) Genome sequence of the human malaria parasite *Plasmodium falciparum*. *Nature* **419**, 498–511 https://doi.org/10.1038/nature01097

36   McRobert, L. and McConkey, G.A. (2002) Rna interference (Rnai) inhibits growth of *Plasmodium falciparum*. *Mol. Biochem. Parasitol.* **119**, 273–278 https://doi.org/10.1016/S0166-6851(01)00429-7

37   Phillips, M.A., Lotharius, J., Marsh, K., White, J., Dayan, A., White, K.L. et al. (2015) A long-Duration dihydroorotate dehydrogenase inhibitor (Dsm265) for prevention and treatment of malaria. *Sci. Transl. Med.* **7**, 296ra111 https://doi.org/10.1126/scitranslmed.aaa6645

38   Fagan, R.L., Nelson, M.N., Pagano, P.M. and Palfey, B.A. (2006) Mechanism of flavin reduction in class 2 dihydroorotate dehydrogenases. *Biochemistry* **45**, 14926–14932 https://doi.org/10.1021/bi060919g

39   Hoelz, L.V.B., Calil, F.A., Nonato, M.C., Pinheiro, L.C.S. and Boechat, N. (2018) *Plasmodium falciparum* dihydroorotate dehydrogenase: a drug target against malaria. *Future Med. Chem.* **10**, 1853–1874 https://doi.org/10.4155/fmc-2017-0250

40   Phillips, M.A. and Rathod, P.K. (2010) Plasmodium dihydroorotate dehydrogenase: a promising target for novel anti-malarial chemotherapy. *Infect. Disord. Drug Targets* **10**, 226–239 https://doi.org/10.2174/187152610791163336

41   Hurt, D.E., Widom, J. and Clardy, J. (2006) Structure of *Plasmodium falciparum* dihydroorotate dehydrogenase with a bound inhibitor. *Acta Crystallogr. D Biol. Crystallogr.* **62**, 312–323 https://doi.org/10.1107/s0907444905042642

42   Walse, B., Dufe, V.T., Svensson, B., Fritzson, I., Dahlberg, L., Khairoullina, A. et al. (2008) The structures of human dihydroorotate dehydrogenase with and without inhibitor reveal conformational flexibility in the inhibitor and substrate binding sites. *Biochemistry* **47**, 8929–8936 https://doi.org/10.1021/bi8003318

43   Malmquist, N.A., Gujjar, R., Rathod, P.K. and Phillips, M.A. (2008) Analysis of flavin oxidation and electron-transfer inhibition in *Plasmodium falciparum* dihydroorotate dehydrogenase. *Biochemistry* **47**, 2466–2475 https://doi.org/10.1021/bi702218c

44   Deng, X., Gujjar, R., El Mazouni, F., Kaminsky, W., Malmquist, N.A., Goldsmith, E.J. et al. (2009) Structural plasticity of malaria dihydroorotate dehydrogenase allows selective binding of diverse chemical scaffolds. *J. Biol. Chem.* **284**, 26999–27009 https://doi.org/10.1074/jbc.m109.028589

45   Baldwin, J., Farajallah, A., Malmquist, N., Rathod, P. and Phillips, M. (2002) Malarial dihydroorotate dehydrogenase: substrate and inhibitor specificity. *J. Biol. Chem.* **277**, 41827–41834 https://doi.org/10.1074/jbc.M206854200

46   Boa, A.N., Canavan, S.P., Hirst, P.R., Ramsey, C., Stead, A.M.W. and McConkey, G.A. (2005) Synthesis of Brequinar analogue inhibitors of malaria parasite dihydroorotate dehydrogenase. *Bioorg. Med. Chem.* **13**, 1945–1967 https://doi.org/10.1016/j.bmc.2005.01.017

47   Baldwin, J., Michnoff, C.H., Malmquist, N.A., White, J., Roth, M.G., Rathod, P.K. et al. (2005) High-throughput screening for potent and selective inhibitors of *Plasmodium falciparum* dihydroorotate dehydrogenase. *J. Biol. Chem.* **280**, 21847–21853 https://doi.org/10.1074/jbc.m501100200

48   Davies, M., Heikkilä, T., McConkey, G.A., Fishwick, C.W.G., Parsons, M.R. and Johnson, A.P. (2009) Structure-Based design, synthesis, and characterization of inhibitors of human and *Plasmodium falciparum* dihydroorotate dehydrogenases. *J. Med. Chem.* **52**, 2683–2693 https://doi.org/10.1021/jm800963t

49   Liu, S., Neidhardt, E.A., Grossman, T.H., Ocain, T. and Clardy, J. (2000) Structures of human dihydroorotate dehydrogenase in complex with antiproliferative agents. *Structure* **8**, 25–33 https://doi.org/10.1016/S0969-2126(00)00077-0

50   Heikkilä, T., Thirumalairajan, S., Davies, M., Parsons, M.R., McConkey, A.G., Fishwick, C.W.G. et al. (2006) The first De novo designed inhibitors of *Plasmodium falciparum* dihydroorotate dehydrogenase. *Bioorg. Med. Chem. Lett.* **16**, 88–92 https://doi.org/10.1016/j.bmcl.2005.09.045

51   Heikkilä, T., Ramsey, C., Davies, M., Galtier, C., Stead, A.M.W., Johnson, A.P. et al. (2007) Design and synthesis of potent inhibitors of the malaria parasite dihydroorotate dehydrogenase. *J. Med. Chem.* **50**, 186–191 https://doi.org/10.1021/jm060687j

52   Patel, V., Booker, M., Kramer, M., Ross, L., Celatka, C.A., Kennedy, L.M. et al. (2008) Identification and characterization of small molecule inhibitors of *Plasmodium falciparum* dihydroorotate dehydrogenase. *J. Biol. Chem.* **283**, 35078–35085 https://doi.org/10.1074/jbc.M804990200

53   Tseng, T.-S., Lee, Y.-C., Hsiao, N.-W., Liu, Y.-R. and Tsai, K.-C. (2016) Comparative study between 3d-Qsar and docking-Based pharmacophore models for potent *Plasmodium falciparum* dihydroorotate dehydrogenase inhibitors. *Bioorg. Med. Chem. Lett.* **26**, 265–271 https://doi.org/10.1016/j.bmcl.2015.12.043

54   Cowen, D., Bedingfield, P., McConkey, G.A., Fishwick, C.W.G. and Johnson, A.P. (2010) A study of the effects of substituents on the selectivity of the binding of N-arylaminomethylene malonate inhibitors to Dhodh. *Bioorg. Med. Chem. Lett.* **20**, 1284–1287 https://doi.org/10.1016/j.bmcl.2009.11.079

55   Pavadai, E., El Mazouni, F., Wittlin, S., de Kock, C., Phillips, M.A. and Chibale, K. (2016) Identification of new human malaria parasite *Plasmodium falciparum* dihydroorotate dehydrogenase inhibitors by pharmacophore and structure-based virtual screening. *J. Chem. Inf. Model.* **56**, 548–562 https://doi.org/10.1021/acs.jcim.5b00680

56   Booker, M.L., Bastos, C.M., Kramer, M.L., Barker, Jr, R.H., Skerlj, R., Sidhu, A.B. et al. (2010) Novel inhibitors of *Plasmodium falciparum* dihydroorotate dehydrogenase with anti-Malarial activity in the mouse model. *J. Biol. Chem.* **285**, 33054–33064 https://doi.org/10.1074/jbc.M110.162081

57   Skerlj, R.T., Bastos, C.M., Booker, M.L., Kramer, M.L., Barker, R.H., Celatka, C.A. et al. (2011) Optimization of potent inhibitors of *P. falciparum* dihydroorotate dehydrogenase for the treatment of malaria. *ACS Med. Chem. Lett.* **2**, 708–713 https://doi.org/10.1021/ml200143c

58   Lukens, A.K., Ross, L.S., Heidebrecht, R., Javier Gamo, F., Lafuente-Monasterio, M.J., Booker, M.L. et al. (2014) Harnessing evolutionary fitness in *Plasmodium falciparum* for drug discovery and suppressing resistance. *Proc. Natl Acad. Sci. U.S.A.* **111**, 799–804 https://doi.org/10.1073/pnas.1320886110

59   Kokkonda, S., Deng, X., White, K.L., El Mazouni, F., White, J., Shackleford, D.M. et al. (2020) Lead optimization of a pyrrole-Based dihydroorotate dehydrogenase inhibitor series for the treatment of malaria. *J. Med. Chem.* **63**, 4929–4956 https://doi.org/10.1021/acs.jmedchem.0c00311

60   Gujjar, R., Marwaha, A., El Mazouni, F., White, J., White, K.L., Creason, S. et al. (2009) Identification of a metabolically stable triazolopyrimidine-based dihydroorotate dehydrogenase inhibitor with antimalarial activity in mice. *J. Med. Chem.* **52**, 1864–1872 https://doi.org/10.1021/jm801343r

61   Gujjar, R., El Mazouni, F., White, K.L., White, J., Creason, S., Shackleford, D.M. et al. (2011) Lead optimization of aryl and aralkyl amine-Based triazolopyrimidine inhibitors of *Plasmodium falciparum* dihydroorotate dehydrogenase with antimalarial activity in mice. *J. Med. Chem.* **54**, 3935–3949 https://doi.org/10.1021/jm200265b

62   Phillips, M.A., White, K.L., Kokkonda, S., Deng, X., White, J., El Mazouni, F. et al. (2016) A triazolopyrimidine-based dihydroorotate dehydrogenase inhibitor with improved drug-Like properties for treatment and prevention of malaria. *ACS Infect. Dis.* **2**, 945–957 https://doi.org/10.1021/acsinfecdis.6b00144

63   Lynch, J.J., Rossignol, E., Moehrle, J.J., Van Vleet, T.R., Marsh, K.C., Parman, T. et al. (2019) Increased stress associated with head-out plethysmography testing can exacerbate respiratory effects and lead to mortality in rats. *J. Pharmacol. Toxicol. Methods* **99**, 106580 https://doi.org/10.1016/j.vascn.2019.106580

64   Coteron, J.M., Marco, M., Esquivias, J., Deng, X., White, K.L., White, J. et al. (2011) Structure-Guided lead optimization of triazolopyrimidine-Ring substituents identifies potent *Plasmodium falciparum* dihydroorotate dehydrogenase inhibitors with clinical candidate potential. *J. Med. Chem.* **54**, 5540–5561 https://doi.org/10.1021/jm200592f

65   Llanos-Cuentas, A., Casapia, M., Chuquiyauri, R., Hinojosa, J.-C., Kerr, N., Rosario, M. et al. (2018) Antimalarial activity of single-dose Dsm265, a novel plasmodium dihydroorotate dehydrogenase inhibitor, in patients with uncomplicated *Plasmodium falciparum* or plasmodium vivax malaria infection: a proof-of-Concept, open-label, phase 2a study. *Lancet Infect. Dis.* **18**, 874–883 https://doi.org/10.1016/S1473-3099(18)30309-8

66   McCarthy, J.S., Rückle, T., Elliott, S.L., Ballard, E., Collins, K.A., Marquart, L. et al. (2019) A single-dose combination study with the experimental antimalarials artefenomel and Dsm265 to determine safety and antimalarial activity against blood-stage *Plasmodium falciparum* in healthy volunteers. *Antimicrob. Agents Chemother.* **64**, e01371–e01319 https://doi.org/10.1128/AAC.01371-19

67   Murphy, S.C., Duke, E.R., Shipman, K.J., Jensen, R.L., Fong, Y., Ferguson, S. et al. (2017) A randomized trial evaluating the prophylactic activity of Dsm265 against preerythrocytic *Plasmodium falciparum* infection during controlled human malarial infection by mosquito bites and direct venous inoculation. *J. Infect. Dis.* **217**, 693–702 https://doi.org/10.1093/infdis/jix613

68   Sulyok, M., Rückle, T., Roth, A., Mürbeth, R.E., Chalon, S., Kerr, N. et al. (2017) Dsm265 for *Plasmodium falciparum* chemoprophylaxis: a randomised, double blinded, phase 1 trial with controlled human malaria infection. *Lancet Infect. Dis.* **17**, 636–644 https://doi.org/10.1016/S1473-3099(17)30139-1

69   Kokkonda, S., El Mazouni, F., White, K.L., White, J., Shackleford, D.M., Lafuente-Monasterio, M.J. et al. (2018) Isoxazolopyrimidine-based inhibitors of *Plasmodium falciparum* dihydroorotate dehydrogenase with antimalarial activity. *ACS Omega* **3**, 9227–9240 https://doi.org/10.1021/acsomega.8b01573

70   Xu, M., Zhu, J., Diao, Y., Zhou, H., Ren, X., Sun, D. et al. (2013) Novel selective and potent inhibitors of malaria parasite dihydroorotate dehydrogenase: discovery and optimization of dihydrothiophenone derivatives. *J. Med. Chem.* **56**, 7911–7924 https://doi.org/10.1021/jm400938g

71   Xu, L., Li, W.J., Diao, Y.Y., Sun, H.X., Li, H.L., Zhu, L.L. et al. (2018) Synthesis, design, and structure-activity relationship of the pyrimidone derivatives as novel selective inhibitors of *Plasmodium falciparum* dihydroorotate dehydrogenase. *Molecules* **23**, 1254 https://doi.org/10.3390/molecules23061254

72   Fritzson, I., Bedingfield, P.T.P., Sundin, A.P., McConkey, G. and Nilsson, U.J. (2011) N-substituted salicylamides as selective malaria parasite dihydroorotate dehydrogenase inhibitors. *Med. Chem. Commun.* **2**, 895–898 https://doi.org/10.1039/C1MD00118C

73   Pippione, A.C., Sainas, S., Goyal, P., Fritzson, I., Cassiano, G.C., Giraudo, A. et al. (2019) Hydroxyazole scaffold-based *Plasmodium falciparum* dihydroorotate dehydrogenase inhibitors: synthesis, biological evaluation and X-ray structural studies. *Eur. J. Med. Chem.* **163**, 266–280 https://doi.org/10.1016/j.ejmech.2018.11.044

74   McGowan, S., Porter, C.J., Lowther, J., Stack, C.M., Golding, S.J., Skinner-Adams, T.S. et al. (2009) Structural basis for the inhibition of the essential *Plasmodium falciparum* M1 neutral aminopeptidase. *Proc. Natl Acad. Sci. U.S.A.* **106**, 2537–2542 https://doi.org/10.1073/pnas.0807398106

75   Skinner-Adams, T.S., Stack, C.M., Trenholme, K.R., Brown, C.L., Grembecka, J., Lowther, J. et al. (2010) Plasmodium falciparum neutral aminopeptidases: new targets for anti-Malarials. *Trends Biochem. Sci.* **35**, 53–61 https://doi.org/10.1016/j.tibs.2009.08.004

76   Paiardini, A., Bamert, R.S., Kannan-Sivaraman, K., Drinkwater, N., Mistry, S.N., Scammells, P.J. et al. (2015) Screening the medicines for malaria venture "Malaria Box" against the *Plasmodium falciparum* aminopeptidases, M1, M17 and M18. *PLoS ONE* **10**, e0115859 https://doi.org/10.1371/journal.pone.0115859

77   Jones, P.M., Robinson, M.W., Dalton, J.P. and George, A.M. (2011) The *Plasmodium falciparum* malaria M1 alanyl aminopeptidase (Pfa-M1): insights of catalytic mechanism and function from Md simulations. *PLoS ONE* **6**, e28589 https://doi.org/10.1371/journal.pone.0028589

78   Klemba, M., Gluzman, I. and Goldberg, D.E. (2004) A plasmodium falciparum dipeptidyl aminopeptidase I participates in vacuolar hemoglobin degradation. *J. Biol. Chem.* **279**, 43000–43007 https://doi.org/10.1074/jbc.M408123200

79   Harbut, M.B., Velmourougane, G., Dalal, S., Reiss, G., Whisstock, J.C., Onder, O. et al. (2011) Bestatin-based chemical biology strategy reveals distinct roles for malaria M1- and M17-family aminopeptidases. *Proc. Natl Acad. Sci. U.S.A.* **108**, E526–E534 https://doi.org/10.1073/pnas.1105601108

80   Rosenthal, P., Sijwali, P., Singh, A. and Shenai, B. (2002) Cysteine proteases of malaria parasites: targets for chemotherapy. *Curr. Pharm. Des.* **8**, 1659–1672 https://doi.org/10.2174/1381612023394197

81   McGowan, S. (2013) Working in concert: the metalloaminopeptidases from *Plasmodium falciparum*. *Curr. Opin. Struct. Biol.* **23**, 828–835 https://doi.org/10.1016/j.sbi.2013.07.015

82   Ragheb, D., Dalal, S., Bompiani, K.M., Ray, W.K. and Klemba, M. (2011) Distribution and biochemical properties of an M1-Family aminopeptidase in *Plasmodium falciparum* indicate a role in vacuolar hemoglobin catabolism. *J. Biol. Chem.* **286**, 27255–27265 https://doi.org/10.1074/jbc.M111.225318

83   Poreba, M., McGowan, S., Skinner-Adams, T.S., Trenholme, K.R., Gardiner, D.L., Whisstock, J.C. et al. (2012) Fingerprinting the substrate specificity of M1 and M17 aminopeptidases of human malaria, *Plasmodium falciparum*. *PLoS ONE* **7**, e31938 https://doi.org/10.1371/journal.pone.0031938

84   Skinner-Adams, T.S., Lowther, J., Teuscher, F., Stack, C.M., Grembecka, J., Mucha, A. et al. (2007) Identification of phosphinate dipeptide analog inhibitors directed against the *Plasmodium falciparum* M17 leucine aminopeptidase as lead antimalarial compounds. *J. Med. Chem.* **50**, 6024–6031 https://doi.org/10.1021/jm070733v

85   Skinner-Adams, T.S., Peatey, C.L., Anderson, K., Trenholme, K.R., Krige, D., Brown, C.L. et al. (2012) The aminopeptidase inhibitor Chr-2863 is an orally bioavailable inhibitor of murine malaria. *Antimicrob. Agents Chemother.* **56**, 3244–3249 https://doi.org/10.1128/AAC.06245-11

86   Velmourougane, G., Harbut, M.B., Dalal, S., McGowan, S., Oellig, C.A., Meinhardt, N. et al. (2011) Synthesis of New (-)-Bestatin-based inhibitor libraries reveals a novel binding mode in the S1 pocket of the essential malaria M1 metalloaminopeptidase. *J. Med. Chem.* **54**, 1655–1666 https://doi.org/10.1021/jm101227t

87   González-Bacerio, J., Maluf, S.E.C., Méndez, Y., Pascual, I., Florent, I., Melo, P.M.S. et al. (2017) Kbe009: an antimalarial bestatin-like inhibitor of the *Plasmodium falciparum* M1 aminopeptidase discovered in an Ugi multicomponent reaction-derived peptidomimetic library. *Bioorg. Med. Chem.* **25**, 4628–4636 https://doi.org/10.1016/j.bmc.2017.06.047

88   Grembecka, J., Mucha, A., Cierpicki, T. and Kafarski, P. (2003) The most potent organophosphorus inhibitors of leucine aminopeptidase. Structure-based design, chemistry, and activity. *J. Med. Chem.* **46**, 2641–2655 https://doi.org/10.1021/jm030795v

89   Sivaraman, K., Paiardini, A., Sienczyk, M., Rugger, C., Oellig, C., Dalton, J.P. et al. (2013) Synthesis and structure-activity relationships of phosphonic arginine mimetics as inhibitors of the M1 and M17 aminopeptidases from *Plasmodium falciparum*. *J. Med. Chem.* **56**, 5213–5217 https://doi.org/10.1021/jm4005972

90   Flipo, M., Beghyn, T., Charton, J., Leroux, V.A., Deprez, B.P. and Deprez-Poulain, R.F. (2007) A library of novel hydroxamic acids targeting the metallo-Protease family: design, parallel synthesis and screening. *Bioorg. Med. Chem.* **15**, 63–76 https://doi.org/10.1016/j.bmc.2006.10.010

91   Flipo, M., Beghyn, T., Leroux, V., Florent, I., Deprez, B.P. and Deprez-Poulain, R.F. (2007) Novel selective inhibitors of the zinc plasmodial aminopeptidase Pfa-M1 as potential antimalarial agents. *J. Med. Chem.* **50**, 1322–1334 https://doi.org/10.1021/jm061169b

92   Flipo, M., Charton, J., Hocine, A., Dassonneville, S., Deprez, B. and Deprez-Poulain, R. (2009) Hydroxamates: relationships between structure and plasma stability. *J. Med. Chem.* **52**, 6790 https://doi.org/10.1021/jm900648x

93   Mistry, S., Drinkwater, N., Ruggeri, C., Sivaraman, K., Loganathan, S., Fletcher, S. et al. (2014) Two-pronged attack: dual inhibition of *Plasmodium falciparum* M1 and M17 metalloaminopeptidases by a novel series of hydroxamic acid-based inhibitors. *J. Med. Chem.* **57**, 9168–9183 https://doi.org/10.1021/jm501323a

94   Drinkwater, N., Vinh, N., Mistry, S., Bamert, R., Ruggeri, C., Holleran, J.P. et al. (2016) Potent dual inhibitors of *Plasmodium falciparum* M1 and M17 aminopeptidases through optimization of S1 pocket interactions. *Eur. J. Med. Chem.* **110**, 43–64 https://doi.org/10.1016/j.ejmech.2016.01.015

95   Vinh, N.B., Drinkwater, N., Malcolm, T.R., Kassiou, M., Lucantoni, L., Grin, P.M. et al. (2019) Hydroxamic acid inhibitors provide cross-species inhibition of plasmodium M1 and M17 aminopeptidases. *J. Med. Chem.* **62**, 622–640 https://doi.org/10.1021/acs.jmedchem.8b01310

96   Salomon, E., Schmitt, M., Marapaka, A.K., Stamogiannos, A., Revelant, G., Schmitt, C. et al. (2018) Aminobenzosuberone scaffold as a modular chemical tool for the inhibition of therapeutically relevant M1 aminopeptidases. *Molecules* **23**, 2607 https://doi.org/10.3390/molecules23102607

97   Salomon, E., Schmitt, M., Mouray, E., McEwen, A.G., Bounaadja, L., Torchy, M. et al. (2020) Aminobenzosuberone derivatives as Pfa-M1 inhibitors: molecular recognition and antiplasmodial evaluation. *Bioorg. Chem.* **98**, 103750 https://doi.org/10.1016/j.bioorg.2020.103750

98   Bounaadja, L., Schmitt, M., Albrecht, S., Mouray, E., Tarnus, C. and Florent, I. (2017) Selective inhibition of Pfa-M1, over Pfa-M17, by an amino-Benzosuberone derivative blocks malaria parasites development in vitro and in vivo. *Malar. J.* **16**, 382 https://doi.org/10.1186/s12936-017-2032-4

99   Dalal, S., Ragheb, D.R.T. and Klemba, M. (2012) Engagement of the S1, S1′ and S2′ subsites drives efficient catalysis of peptide bond hydrolysis by the M1-Family aminopeptidase from *Plasmodium falciparum*. *Mol. Biochem. Parasitol.* **183**, 70–77 https://doi.org/10.1016/j.molbiopara.2012.02.003

100   Deprez-Poulain, R., Flipo, M., Piveteau, C., Leroux, F., Dassonneville, S., Florent, I. et al. (2012) Structure-activity relationships and blood distribution of antiplasmodial aminopeptidase-1 inhibitors. *J. Med. Chem.* **55**, 10909–10917 https://doi.org/10.1021/jm301506h

101   Yang, W., Riley, B.T., Lei, X., Porebski, B.T., Kass, I., Buckle, A.M. et al. (2018) Mapping the pathway and dynamics of bestatin inhibition of the *Plasmodium falciparum* M1 aminopeptidase *Pf*A-M1. *ChemMedChem* **13**, 2504–2513 https://doi.org/10.1002/cmdc.201800563